Influence of global coupling through the gas phase on the dynamics of CO oxidation on Pt(110)

M. Falcke and H. Engel
Institut für Theoretische Physik, AG "Dissipative Strukturen," Technische Universität Berlin, Rudower Chaussee 5, Geb. 2.14, 12489 Berlin, Germany
(Received 24 September 1993)

In CO oxidation on platinum single-crystal surfaces spatial coupling takes place via two basic mechanisms: locally by surface diffusion of mobile adsorbates and globally by pressure changes in the gas phase. The effect of these two competing coupling modes on the dynamics of the reaction is studied using a reaction-diffusion model supplemented by an equation for the balance of the partial pressure of CO in the gas phase. The integral reaction rate and the associated spatiotemporal patterns of CO coverage show strong influence of coupling through the gas phase.

PACS number(s): 82.20.Wt, 82.20.Mj, 82.65.Jv

INTRODUCTION

Apart from the Belousov-Zhabotinsky reaction many other chemical reactions exhibit spontaneous spatiotemporal structure formation under far from equilibrium conditions. For example, with the CO oxidation on platinum single-crystal surfaces under low-pressure conditions, in measurements with high spatial resolution using photoemission electron microscopy a wide range of spatial patterns and wave phenomena has been observed [1,2]. In this system spatial coupling is realized via two basic mechanisms: locally by surface diffusion of mobile adsorbates (predominantly of adsorbed CO) and globally by pressure changes in the gas phase.

The aim of this paper is to study how global coupling may affect integral behavior and pattern formation in the reaction-diffusion system. We address the reader to Ref. [3] for detailed information about the underlying mechanism of the reaction. The variables of the model are the coverages of carbon monoxide (c), of oxygen (o), and the fraction of the unreconstructed surface (w) which obey the following system of equations:

$$\frac{\partial c}{\partial t}=D_1\frac{\partial^2 c}{\partial r_1^2}+\frac{\partial}{\partial r_2}\left[D_2(w)\frac{\partial c}{\partial r_2}\right]+k_1 p_{CO} s_c\left[1-\left[\frac{c}{c_s}\right]^3\right]-k_2 c-k_3 co\ , \tag{1}$$

$$\frac{\partial o}{\partial t}=k_4 p_{O2}[w s_{O1}+(1-w)s_{O2}]\left[1-\frac{c}{c_s}-\frac{o}{o_s}\right]^2-k_3 co\ , \tag{2}$$

$$\frac{\partial w}{\partial t}=k_5\times\begin{cases}-w, & 0\le\dfrac{c}{c_s}<0.2\\ -w-\dfrac{\left[\dfrac{c}{c_s}\right]^3-1.05\left[\dfrac{c}{c_s}\right]^2+0.3\dfrac{c}{c_s}-0.026}{0.0135}, & 0.2\le\dfrac{c}{c_s}\le 0.5\\ -w+1, & 0.5<\dfrac{c}{c_s}\le 1.0\end{cases}$$
$$=k_5\left[f\left[\frac{c}{c_s}\right]-w\right]\ . \tag{3}$$

The first equation describes changes in the CO coverage due to anisotropy surface diffusion (D_1 and D_2 are the diffusion coefficients in the $[1\bar{1}0]$ resp. [001] crystallographic orientation), adsorption, desorption, and reaction. The equation for the dynamics of adsorbed oxygen considers adsorption and reaction; desorption and diffusion of adsorbed oxygen are negligible in the temperature range considered. Note that the oxygen sticking coefficient is taken as sum of the values for the 1×1 and the reconstructed 1×2 phase of the surface structure. The fraction of the unreconstructed surface obeys Eq. (3) which describes the adsorbate-induced structural phase transition of the Pt(110) surface. The kinetic scheme [Eqs. (1)–(3) with $D_1=D_2=0$, the so-called reconstruction model of surface oscillations] is thoroughly analyzed in [3]. For convenience, the meaning and the values of all

TABLE I. Parameters of the model; here $k_i = A_i \exp(-E_i/RT)$.

CO	k_1	Adsorption rate	4.18×10^5 s^{-1}Torr^{-1}
	s_c	Sticking coefficient	1
	c_s	Saturation coverage	1
O_2	k_4	Rate of O hitting surface	7.81×10^5 s^{-1}Torr^{-1}
	s_{O1}	Sticking coefficient on 1×1	0.6
	s_{O2}	Sticking coefficient on 1×2	0.4
	o_s	Saturation coverage	0.8
Rates	k_3	Reaction	$A_3=3\times10^6$ s^{-1}, $E_3=10$ kcal/mol
	k_2	CO desorption	$A_2=2\times10^{16}$ s^{-1}, $E_4=38$ kcal/mol
	k_5	Phase transition	$A_5=10^2$ s^{-1}, $E_5=7$ kcal/mol
Diffusion	D_1	Diffusion coefficient in	
	D_2	$[1\bar{1}0]$ resp. [001] direction	
Global coupling	V_{ML}	Volume of one monolayer	
	V	Reactor volume	50 l
	A	Area of the surface	
	J	Gas flow into the reactor	360 l/s
External parameters	p_{CO}	Partial pressure of CO	
	p_{COe}	Partial pressure of CO in the gas inlet	
	p_{O2}	Partial pressure of O_2	
	T	Temperature	545 K

parameters used throughout are given in Table I.

Some comments concerning the diffusion term in Eq. (2) need to be added. The 1×1 and the 1×2 configuration of the crystal surface differ from each other not only with respect to the sticking coefficient of oxygen (which is higher for the unreconstructed surface) but also with respect to diffusion of adsorbed CO. For the 1×2 ("missing row") structure, it is known that the diffusion is strongly anisotropic namely by a factor of about 10 faster in the $[1\bar{1}0]$ than in the [001] crystallographic direction. During the reconstruction cycle the surface is partly or totally in the 1×2 configuration. A simple ansatz for the unknown w dependence of D_2 is given by

$$D_2(w)=D_2\left[1+\left[\frac{D_1}{D_2}-1\right]w^3\right]=D_2\rho(w,\eta),\ \eta=\frac{D_1}{D_2}\ . \tag{4}$$

The consequences of surface-state-dependent diffusion of adsorbed CO are beyond the scope of this paper. In global coupling studied here this dependence is considered for completeness.

GAS-PHASE COUPLING

Let us first introduce dimensionless variables according to

$$u=\frac{c}{c_s},\ v=\frac{o}{o_s},\ \tau=k_5t,\ z_1=\frac{k_5 r_i}{\sqrt{D_1 k_1 p_{COe}}}\ ,\quad i=1,2\ . \tag{5}$$

Then we obtain from Eqs. (1)–(4)

$$\varepsilon\frac{\partial u}{\partial\tau}=\varepsilon^2\left[\eta\frac{\partial^2 u}{\partial z_1^2}+\frac{\partial}{\partial z_2}\left[\rho(w,\eta)\frac{\partial u}{\partial z_2}\right]\right]+\nu(1-u^3)-\beta u-\gamma uv\ , \tag{6}$$

$$o_s\varepsilon\frac{\partial v}{\partial\tau}=\delta(w+\sigma)(1-u-v)^2-\gamma uv\ , \tag{7}$$

$$\frac{\partial w}{\partial\tau}=f(u)-w\ , \tag{8}$$

where the abbreviations

$$\varepsilon=\frac{k_5}{k_1 p_{COe}},\ \beta=\frac{k_2}{k_1 p_{COe}},\ \gamma=\frac{k_3 o_s}{k_1 p_{COe}}\ ,$$
$$\delta=\frac{k_4 p_{O2}(s_{O1}-s_{O2})}{k_1 p_{COe}},\ \nu=\frac{p_{CO}}{p_{COe}},\ \sigma=\frac{s_{O2}}{s_{O1}-s_{O2}} \tag{9}$$

are used. Depending on the values of the external, experimentally accessible parameters p_{CO}, p_{o2}, and T the reaction exhibits bistable, excitable, or oscillatory local dynamics. Here we concentrate on the oscillatory regime; for bistable and excitable regime compare [4–6].

We assume that the gas-phase coupling is realized via the partial pressure of CO, and that on the time scale of the reaction pressure changes in the gas-phase equilibrate instantaneously. Therefore, p_{CO} should be treated as an additional variable. The p_{CO} balance

$$\frac{dp_{CO}}{dt}=\frac{J}{V}\left\{p_{COe}-p_{CO}\left[1+\frac{V_{ML}}{JA}\int dr^2[k_1 p_{CO}(1-u^3)-k_2 u]\right]\right\} \quad (10)$$

consists of inflow and outflow as well as of terms due to adsorption and desorption of CO. The two last mentioned contributions are obtained by integrating over the whole crystal surface and multiplying the result with the volume of one monolayer V_{ML} [note that the coverages in Eqs. (1)–(3) are given per one monolayer]. The other parameters used in Eq. (10) denote the volume gas current (J), the volume of the reactor (V), the area of the crystal surface (A), and the CO partial pressure in the gas inlet (p_{COe}).

RESULTS

To elucidate the influence of the two mechanisms of spatial coupling on the dynamics of the reaction, first we consider the integral reaction rate obtained by numerical integration of Eqs. (6)–(10). The calculations were carried out for fixed external conditions, specified by the partial pressure of CO in the gas inlet, the partial pressure of oxygen and the temperature, but at different levels of modeling depending on which mechanism of spatial coupling is taken into account resp. provides the dominant

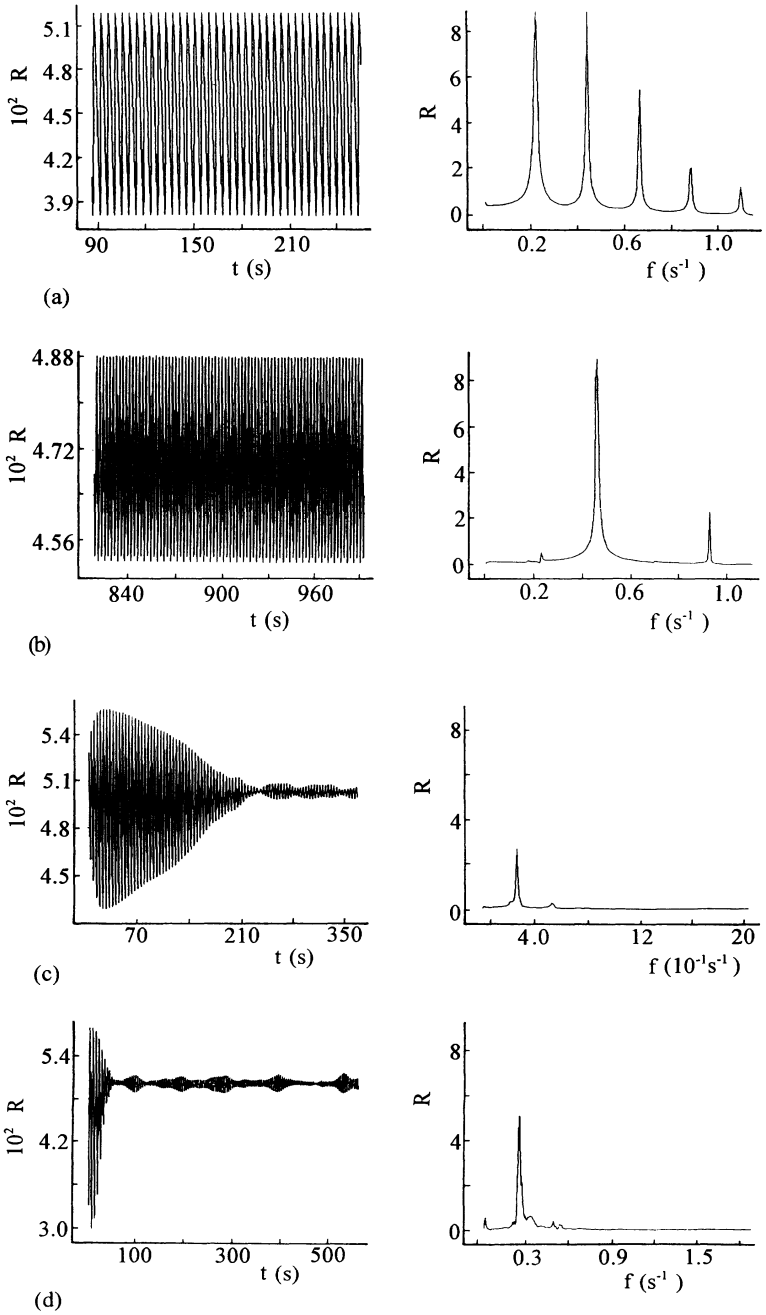

FIG. 1. Integral reaction rate at different levels of modeling: (a) pure kinetic model, $p_{CO}=3.963\times10^{-5}$ Torr, $D_i=0$, $V_{ML}=0$; (b) 1296 individual kinetic oscillators coupled through the gas phase, $p_{COe}=3.992\times10^{-5}$ Torr, $D_i=0$, $V_{ML}=0.225$ l/ML; (c) reaction-diffusion model, $p_{COe}=3.98\times10^{-5}$ Torr, $\eta=8$, $V_{ML}=0$; (d) complete model including local and global coupling, $p_{COe}=3.992\times10^{-5}$ Torr, $\eta=8$, $V_{ML}=0.225$ l/ML. Parameter values of the local dynamics (kinetic model) belong to the oscillatory domain near the Hopf bifurcation: $p_{O2}=1.187\times10^{-4}$ Torr, $T=545$ K. For these parameter values the phase diffusion coefficient of the Kuramoto-Shivashinsky equation is positive [15].

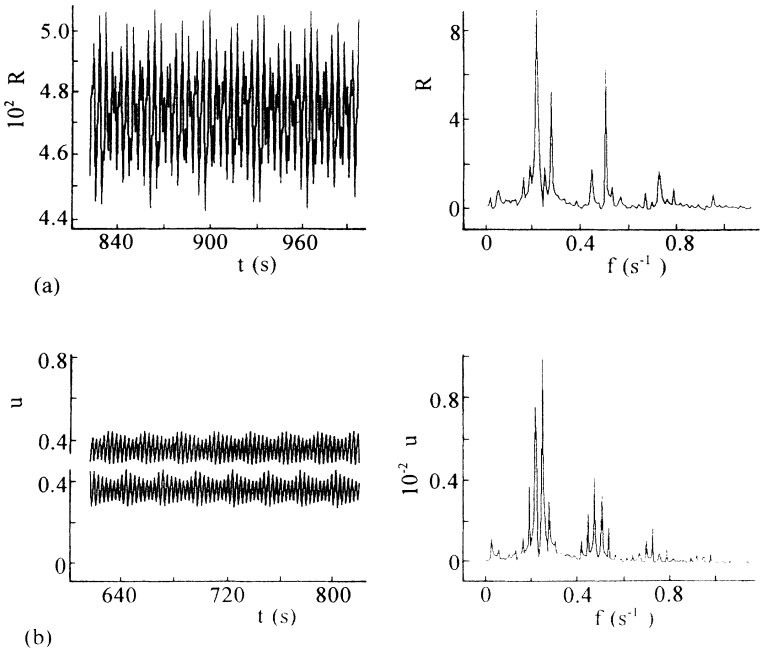

FIG. 2. (a) Time series and Fourier spectrum of 1296 oscillators according to Eqs. (6)–(9) coupled through the gas phase as described by Eq. (10). Parameter values: $p_{COe}=3.992\times10^{-5}$ Torr, $p_{O2}=1.187\times10^{-4}$ Torr, $T=545$ K, $D_i=0$, $V_{ML}=0.3$ l/ML and $J=360$ l/s. In this regime the local CO coverage behaves as shown in (b). Both oscillations have same frequency spectrum but are shifted in phase. The rate in (a) results from a superposition of nearly the same number of oscillators in both of the two clusters.

coupling mode. The details of the numerical procedure are described in Ref. [7].

Figure 1(a) depicts the integral reaction rate that follows from the pure kinetic model, i.e., neglecting both surface diffusion and gas-phase coupling [Eqs. (6)–(9) with $D_1=D_2=0$]. Since the parameter values used for p_{COe}, p_{O2}, and T belong to the oscillatory regime of the reaction near the Hopf bifurcation, the reaction rate exhibits sustained kinetic oscillations.

With gas-phase coupling as the unique spatial coupling mode [Eqs. (6)–(10), $D_1=D_2=0$] we obtain the integral reaction rate presented on Fig. 1(b). The oscillation frequency is about twice as large as in the pure kinetic model. Besides frequency shift gas-phase coupling induces amplitude modulation. A closer inspection reveals that in a certain range of V_{ML} all individual oscillators have the same frequency but they belong to one of two different clusters. Oscillators belonging to the same cluster are locked in phase and there is a constant phase shift between the two clusters. This remarkable effect is shown in Fig. 2. Note the sharp transition from complex small amplitude oscillations to regular large amplitude oscillations when V_{ML} is increased. For the parameter values used in our calculations this transition occurs at about $V_{ML}=0.350\pm0.005$ liter (l)/ML (compare Fig. 3).

For the reaction-diffusion model [Eqs. (6)–(9) with $p_{CO}=p_{COe}=$const] we end up with the integral reaction rate shown in Fig. 1(c). In this case the oscillations have actually nearly the same frequency as in Fig. 1(a) but clearly they are more complex due to many excited modes. Accordingly, the Fourier spectrum of the reaction rate is much broader. The additional peak at small frequency corresponds to amplitude modulations which become stationary after some transient stage. Note again that the amplitude of oscillations is rather small compared to the case of pure gas-phase coupling.

Considering both mechanisms for spatial coupling simultaneously leads to the result shown on Fig. 1(d). Here due to the effect of gas-phase coupling the main peak of the spectrum is again more pronounced and relaxation to the stationary state takes place more rapidly compared to Fig. 1(c). In the integral reaction rate the transition to a globally synchronized state is associated with the emergence of regular, large amplitude oscillations. In Fig. 4(a), this transition occurs at about 170 s after starting from a random initial condition (initial phases are randomly chosen on the limit cycle). Associated patterns of CO coverage are shown in Figs. 4(b) and 4(c). Here 4(b) and 4(c) are snapshots at $t=4.5$ s and $t=220.7$ s, respectively, on the time scale in Fig. 4(a).

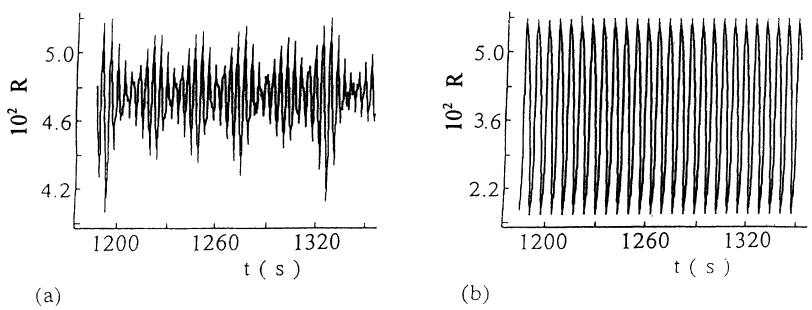

FIG. 3. Time series of the integral reaction rate close to the threshold for the breakdown of global coupling. (a) $V_{ML}=0.3500$ l/ML, (b) $V_{ML}=0.3501$ l/ML. Parameter values; $P_{COe}=3.9975\times10^{-5}$ Torr, $p_{O2}=1.187\times10^{-4}$ Torr, $T=545$ K, $D_i=0$, and $J=360$ l/s.

Obviously, extended homogenized areas are formed on the surface. After sufficiently long time, the whole surface has been transformed into the state of uniform synchronous oscillations. To test whether synchronously oscillating domains are conserved by a weaker gas-phase coupling, the state of the run with $V_{ML}=0.825$ l/ML was continued with $V_{ML}=0.675$ l/ML before homogenization was completed. Neither the large amplitude oscillations of the reaction rate nor the synchronously oscillating domains are maintained under this condition. These domains shrink and finally gas-phase coupling breaks down.

On a time scale large compared to the period of global oscillations, islandlike areas on the platinum surface with

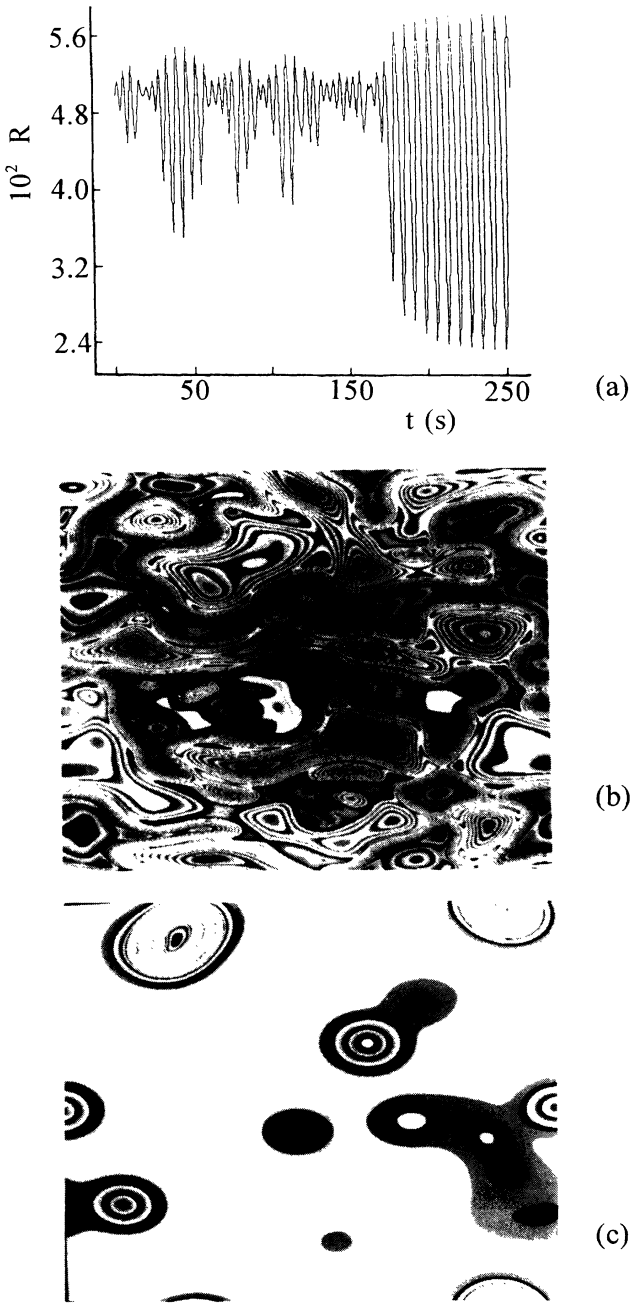

FIG. 4. (a) Integral reaction rate obtained for $V_{ML}=0.825$ l/ML $> V_{ML}^{cr}$ and $p_{CO_e}=4.062\ 10^{-5}$ Torr starting from a random initial phase distribution. The other parameters are the same as in Fig. 3. The snapshots of CO coverage correspond to time moments (b) $t=4.5$ s and (c) $t=220.7$ s; gray levels refer to coverage values.

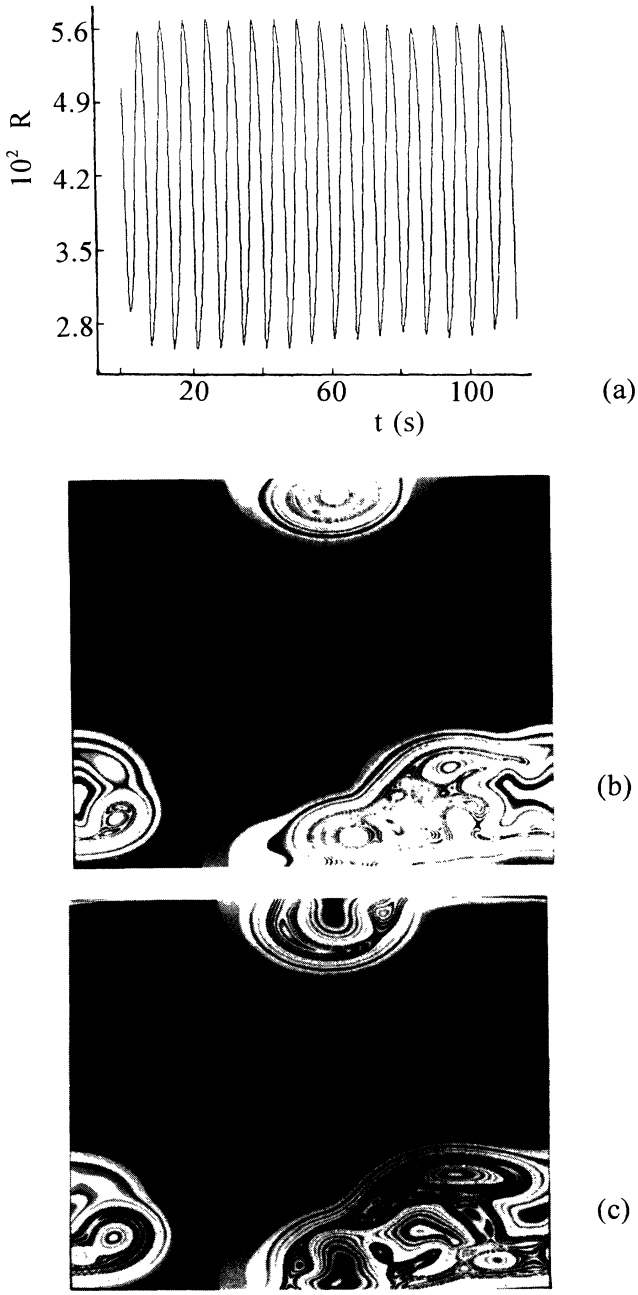

FIG. 5. Island formation on a uniformly oscillating Pt(110) surface. The values of the external parameters $p_{CO_e}=3.992\times10^{-5}$ Torr, $p_{O_2}=1.17\times10^{-4}$ Torr, $T=545$ K correspond to relaxation oscillations of the integral reaction rate. The other parameter values are $D_i=0$, $V_{ML}=0.225$ l/ML, and $J=360$ l/s.

developed spatiotemporal pattern coexist with unstructured domains oscillating synchronously. Within this time scale one island may join with another or disappear. An example for this quasistationary coexistence of surface areas covered with spatiotemporal structures and homogeneously oscillating domains is shown in Fig. 5. The synchronously oscillating domains are phase locked by the global coupling through the gas phase. The structured islands embedded into the oscillating background are composed of phase waves. Sometimes, phase waves are transformed into trigger waves if their velocity becomes smaller than the velocity of the trigger wave at the corresponding values of parameters. Then targetlike wave patterns are formed which are elongated due to anisotropy of surface diffusion.

DISCUSSION

Global coupling through the gas phase is not limited to minor quantitative corrections but may strongly influence the dynamics of the reaction. The numerical simulations indicate that the breakdown of global coupling is a threshold phenomenon. There exists some critical value $V_{\mathrm{ML}}^{\mathrm{cr}}$ such that for $V_{\mathrm{ML}} > V_{\mathrm{ML}}^{\mathrm{cr}}$ the asymptotic state of the system is a spatially uniformly oscillating surface. In the integral reaction rate the breakdown of global coupling appears as the transition from regular oscillations of relatively large amplitude to small amplitude irregular behavior. For $V_{\mathrm{ML}} < V_{\mathrm{ML}}^{\mathrm{cr}}$ the behavior depends on whether there is a local coupling or not. Without surface diffusion, the individual oscillators are separated into two nearly equally occupied clusters. Members of the same cluster oscillate in phase. Between the clusters a fixed phase difference is established. When surface diffusion is included cluster formation may be observed at least very close to the Hopf bifurcation of the system described by Eqs. (1)–(3).

Theoretically, the effects of global coupling in oscillatory media are studied adding global coupling terms to the complex Ginzburg-Landau equation (GLE) for the complex oscillation amplitude. This analysis is restricted to the vicinity of the Hopf bifurcation where oscillations are almost harmonical and their amplitudes are relatively small. In Ref. [8] the additional term is a given external periodic driving force. Mertens, Imbihl, and Mikhailov consider the case where the additional term in the GLE is proportional to the spatial average of the local oscillation amplitudes. It is shown that global coupling can induce its own breakdown [9]. This conclusion is in agreement with our results obtained by numerical simulation of the reaction-diffusion equations. Hakim and Rappel [10] use a discrete version of the complex GLE describing an ensemble of globally coupled limit cycle oscillators without local coupling. Among other dynamic regimes they observe a breaking of the ensemble into a few macroscopic clusters which can exhibit periodic or quasiperiodic behavior. Our findings about separation of local oscillators into clusters, which under local coupling can organize synchronously oscillating spatial domains on the catalytically active surface, correspond directly to the result of these authors.

Partly, the evolution of the coverage pattern reminds us of a scenario for the breakdown of global coupling in the NO+CO reaction on Pt(100) reported by Veser *et al.* [11]. Once locally a space-time structure has established on the surface, in that domain the influence of global coupling is diminished. This favors the formation of additional structured islands that in turn diminish the global coupling further and so forth. Thus when the strength of global coupling allows for the formation of localized structures, a self-accelerating process starts which ends up with a globally desynchronized state.

Finally we emphasize that oscillations in the partial pressure of CO during the reaction have been observed experimentally [12]. In a parameter range where global coupling through the gas phase provides the dominant coupling mode, experimental data for the reaction rate should be compared to a model that explicitly treats p_{CO} as an independent dynamic variable rather than as a fixed external parameter. Our results suggest that global coupling may be responsible for a transition from homogeneous oscillations (V_{ML} sufficiently large) to complex temporal behavior (V_{ML} below $V_{\mathrm{ML}}^{\mathrm{cr}}$). For CO oxidation on Pt(110), a period-doubling transition to chaos [3,13] and even hyperchaos [14] was observed. Up to now, these phenomena were related to additional processes on the surface. Global coupling through the gas phase might provide an alternative mechanism for the explanation of these experimental results.

ACKNOWLEDGMENT

This work was supported by a grant from the Deutsche Forschungsgemeinschaft.

[1] H. H. Rotermund, W. Engel, M. Kordesch, and G. Ertl, Nature (London) **343**, 355 (1990).
[2] S. Jakubith, H. H. Rotermund, W. Engel, A. von Oertzen, and G. Ertl, Phys. Rev. Lett. **65**, 3013 (1990).
[3] K. Krischer, M. Eiswirth, and G. Ertl, J. Chem. Phys. **96**, 9161 (1992).
[4] M. Bär, C. Zülicke, M. Eiswirth, and G. Ertl, J. Chem. Phys. **96**, 8595 (1992).
[5] M. Bär, M. Falcke, C. Zülicke, H. Engel, M. Eiswirth, and G. Ertl, Surf. Sci. **269/270**, 471 (1992).
[6] M. Falcke, M. Bär, H. Engel, and M. Eiswirth, J. Chem. Phys. **97**, 4555 (1992).
[7] M. Falcke, Ph.D. thesis, Humboldt-University, Berlin, 1994.
[8] P. Coullet and K. Emilsson, Physica A **188**, 190 (1992).
[9] F. Mertens, R. Imbihl, and A. S. Mikhailov, J. Chem. Phys. **99**, 8668 (1993).
[10] V. Hakim and W.-J. Rappel, Phys. Rev. A **46**, R7347 (1992).
[11] G. Veser, F. Mertens, A. S. Mikhailov, and R. Imbihl,

Phys. Rev. Lett. **77**, 975 (1993).
[12] M. Eiswirth, P. Möller, K. Wetzl, R. Imbihl, and G. Ertl, J. Chem. Phys. **90**, 510 (1989).
[13] M. Eiswirth, K. Krischer, and G. Ertl, Surf. Sci. **202**, 265 (1988).
[14] M. Eiswirth, Th.-M. Kruel, G. Ertl, and F. W. Schneider, Chem. Phys. Lett. **193**, 305 (1992).
[15] M. Falcke and H. Engel, in *Spatio-temporal Organization in Nonequilibrium Systems,* edited by S. C. Müller and Th. Plesser (Projekt-Verlag, Dortmund, 1992), p. 78.

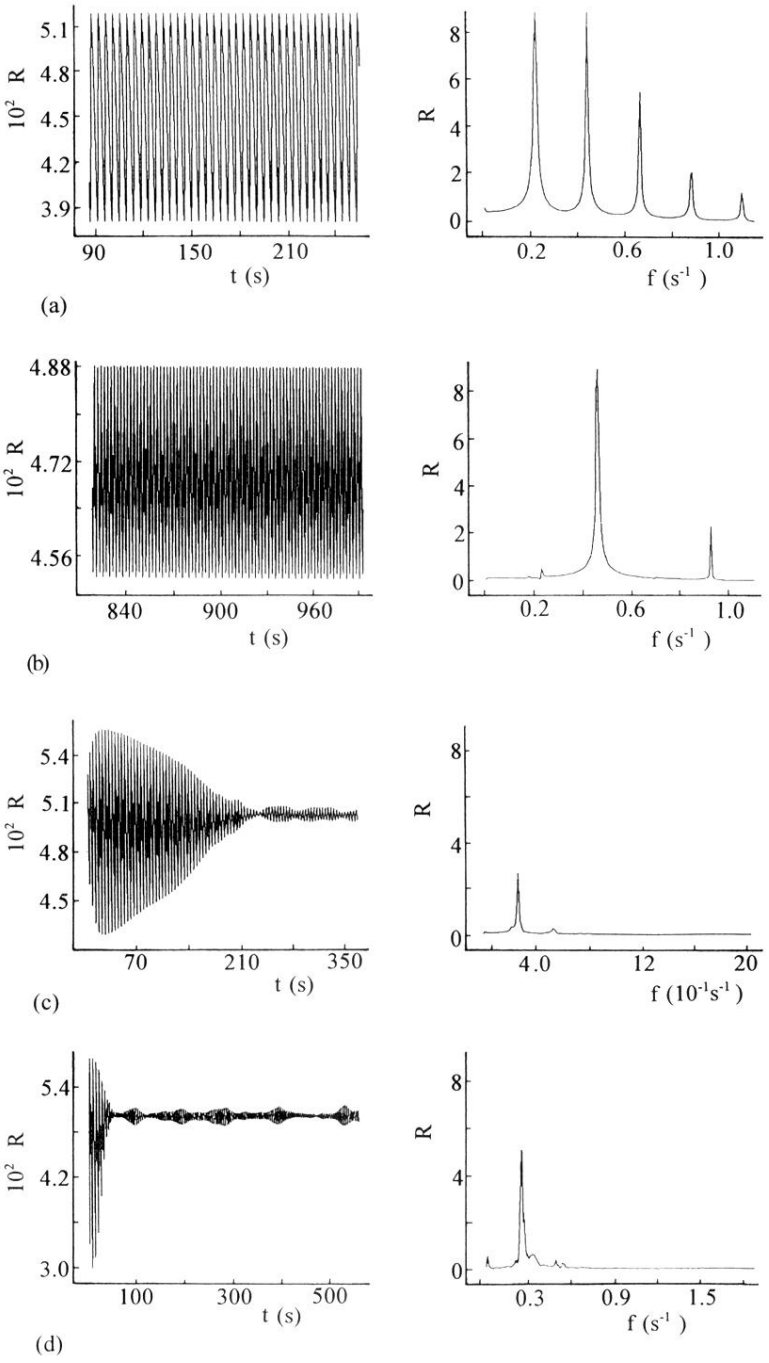

FIG. 1. Integral reaction rate at different levels of modeling: (a) pure kinetic model, $p_{CO}=3.963\times10^{-5}$ Torr, $D_i=0$, $V_{ML}=0$; (b) 1296 individual kinetic oscillators coupled through the gas phase, $p_{COe}=3.992\times10^{-5}$ Torr, $D_i=0$, $V_{ML}=0.225$ l/ML; (c) reaction-diffusion model, $p_{COe}=3.98\times10^{-5}$ Torr, $\eta=8$, $V_{ML}=0$; (d) complete model including local and global coupling, $p_{COe}=3.992\times10^{-5}$ Torr, $\eta=8$, $V_{ML}=0.225$ l/ML. Parameter values of the local dynamics (kinetic model) belong to the oscillatory domain near the Hopf bifurcation: $p_{O2}=1.187\times10^{-4}$ Torr, $T=545$ K. For these parameter values the phase diffusion coefficient of the Kuramoto-Shivashinsky equation is positive [15].

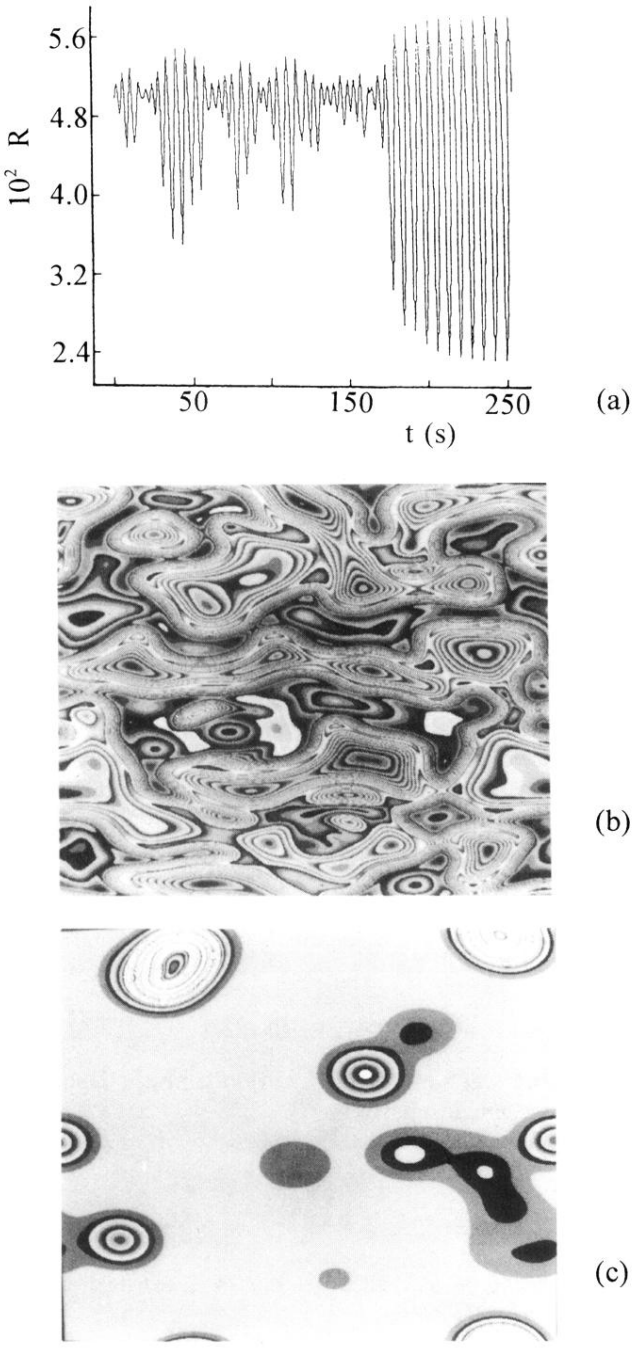

FIG. 4. (a) Integral reaction rate obtained for $V_{ML}=0.825$ l/ML $> V_{ML}^{cr}$ and $p_{COe}=4.062\ 10^{-5}$ Torr starting from a random initial phase distribution. The other parameters are the same as in Fig. 3. The snapshots of CO coverage correspond to time moments (b) $t=4.5$ s and (c) $t=220.7$ s; gray levels refer to coverage values.

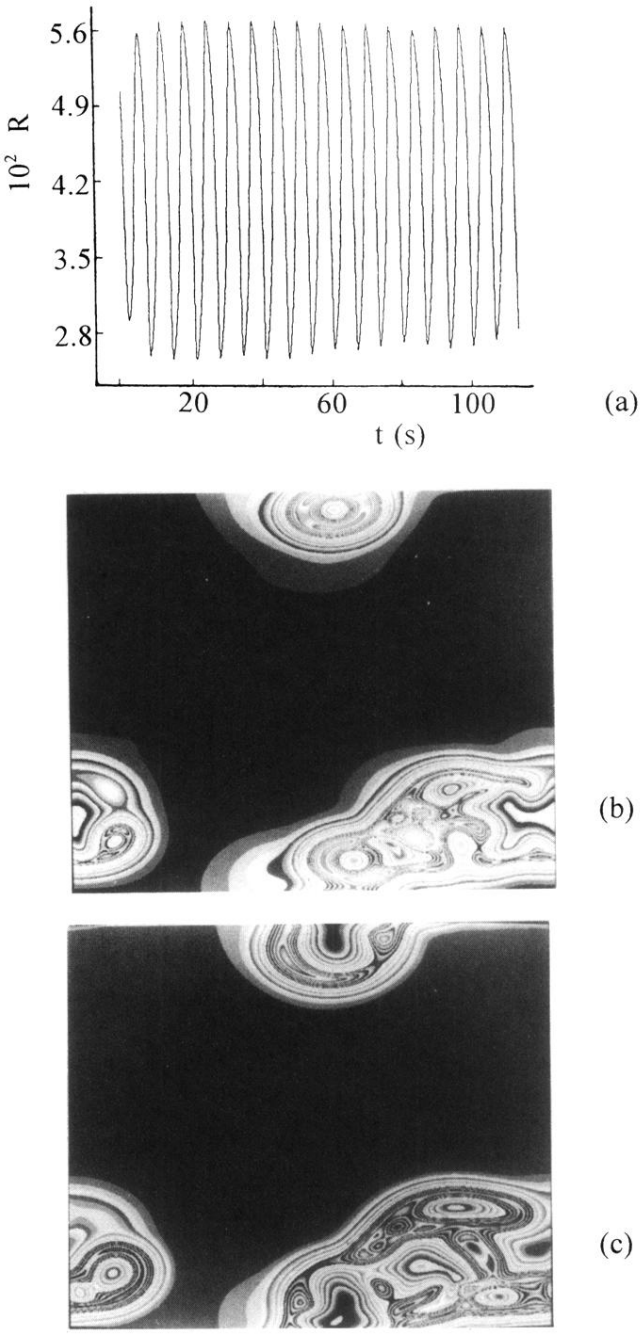

FIG. 5. Island formation on a uniformly oscillating Pt(110) surface. The values of the external parameters $p_{COe}=3.992\times10^{-5}$ Torr, $p_{O2}=1.17\times10^{-4}$ Torr, $T=545$ K correspond to relaxation oscillations of the integral reaction rate. The other parameter values are $D_i=0$, $V_{ML}=0.225$ l/ML, and $J=360$ l/s.